Enrichment of hepatocytes in a HepaRG culture using spatially selective photodynamic treatment

Artur Bednarkiewicz
Robim M. Rodrigues
Maurice P. Whelan
European Commission
Institute of Health and Customer Protection
Via Enrico Fermi 1
Ispra, 21020 Italy

Abstract. The human hepatoma HepaRG cell line is an *in vitro* cell model that is becoming an important tool in drug metabolism, hepatotoxicity, genotoxicity, and enzyme induction studies. The cells are highly proliferative during their undifferentiated state but once committed, they differentiate into two distinctly different cell types, namely, hepatocyte-like and biliary epithelial-like cells. The presence of the latter in the cell culture is considered to be a drawback of the cell model. Since the proliferating undifferentiated HepaRG cells have a bipotent character, the only way to improve the content ratio of hepatic versus biliary cells of differentiated HepaRG cells is to eradicate biliary cells *in situ*, in a way that free surface space does not become available and thus no transdifferentiation can occur. Spatially selective photodynamic therapy has proven to be effective for that purpose. First, all the cells were administered aminolevulinic acid (δ-ALA) to stimulate the synthesis of protoporphyrin IX (PpIX), a naturally occurring photosensitizer. Then, the biliary cells were automatically identified and outlined by bright-field image processing. Last, UV light patterns were projected onto the epithelial cells alone by a spatial light modulation device connected to an optical microscope; therefore, only these cells were destroyed by photodynamic therapy.
 [DOI: 10.1117/1.3369000]

Keywords: HepaRG; cocultures splitting; photodynamic therapy; digital micromirror device.

Paper 09423R received Sep. 21, 2009; revised manuscript received Jan. 20, 2010; accepted for publication Jan. 20, 2010; published online Apr. 2, 2010.

1 Introduction

The human hepatoma HepaRG cell line is an *in vitro* cell model that is becoming an important tool in drug metabolism, hepatotoxicity, genotoxicity, and enzyme induction studies. Although human primary hepatocytes are considered to some extent as the gold standard for hepatic *in vitro* cell models, they have particular limitations such as donor variability, little or no potential to proliferate, limited availability, and phenotypic alterations.[1] On the other hand, immortalized hepatic cell lines often lack the majority of specific hepatic cell functions. The HepaRG model is a possible exception, however, since this cell line demonstrates specific hepatocyte functions that are comparable to primary cultures of human hepatocytes, i.e., expression of most of the phase I and phase II enzymes that are involved in xenobiotic metabolism as well as the constitutive androstane receptors (CARs) and hepatic drug transporters.[1–4]

HepaRG cells are highly proliferative during their undifferentiated state, but once committed, they differentiate into two distinctly different cell types, namely, hepatocyte-like cells and biliary epithelial-like cells.[5] The presence of the biliary epithelial-like cells can be a disadvantage of the cell model in metabolism-mediated cytotoxicity studies since the biliary epithelial cells do not obviously express the hepatic cell functions that make the model so attractive. When selectively isolated and cultured at high density, hepatocytes have been shown to preserve their differentiation state and represent up to 80% of the total cell population.[5] However, biliary epithelial cells will typically be present too. Another problem comes from variability of hepatic cell content from cell to cell and from plate to plate.

Since proliferating undifferentiated HepaRG cells have a bipotent character, the only way to improve the content ratio of hepatic versus biliary cells is to treat the differentiated cell culture in some manner. Cell separation methods to purify a particular cell type from a mixed culture are frequently based on the properties of single cells in suspension, e.g., cell size, cell density, cell granularity, cell surface area, or surface protein configuration.[6] A successful separation will depend on the differences in these characteristics between the different cell types. Subsequently, it is then possible to exclusively culture the obtained purified cell type while the "contaminating" cells are discarded.[6] Unfortunately, this separation approach cannot be used for the purification of hepatocytes in a HepaRG cell culture. The reason for this is intrinsic to the cell model itself. As described earlier, due to the bipotent properties of the HepaRG progenitor cells, the adherent HepaRG cell culture will

Address all correspondence to: Artur Bednarkiewicz, Institute of Low Temperature and Structure Research, Polish Academy of Sciences, Okolna 2, Wroclaw, 50-422 Poland. Tel: 48-71 34-35-021 int. 166; E-mail: a.bednarkiewicz@int.pan.wroc.pl

1083-3668/2010/15(2)/028002/7/$25.00 © 2010 SPIE

always be composed of two morphologically and functionally different cell types. There are no known selective culturing conditions available that would favor hepatic cell growth over biliary epithelial cell proliferation. Therefore, an alternative method to selectively purify the hepatocyte cell fraction is to eliminate biliary epithelial cells *in situ*, in a way that free surface space does not become available and thus no transdifferentiation can occur. As described here, one approach to such *in situ* purification is to selectively destroy biliary cells through spatially controlled photochemically induced necrosis or apoptosis.

Photodynamic therapy (PDT) has proven to selectively and effectively kill tumorous tissues. The clinical applications,[7–13] photosensitizers,[14–19] and photophysical and biological mechanisms[20,21] of this therapeutic method have been extensively studied and reviewed. Basically, PDT relies on the selective accumulation of a photosensitizer (PS) inside the volume of neoplastic cells (or tissue) followed by photoactivation of these photosensitive dyes. Upon illumination, reactive molecules, predominantly singlet oxygen or free radicals, are formed, leading to localized cell death. The mechanisms of cellular death upon PDT treatment strongly depend on the biochemical properties of the photosensitizer as well as on the excitation light dose and wavelength.[7]

One of the most frequently used photosensitizers is protoporphyrin IX (PpIX), which is produced *in situ* by cells after administration of its precursor delta aminolevulinic acid (δ-ALA).[8,9,16] Low concentrations of endogenous δ-ALA also occur naturally in cells, as this molecule is a metabolic precursor of protoporphyrin IX, the penultimate metabolite of the heme biosynthetic pathway and the actual photosensitizer. Under physiological conditions, free heme regulates the cellular heme synthesis in a negative feedback control of the enzyme δ-ALA synthetase. However, when exogenous δ-ALA is added in excess, this control mechanism is bypassed, and PpIX is synthesized in excess, accumulates in the mitochondria of the cells, and by further diffusion all over the cell, renders them photosensitive.

To be effective, PDT requires subsequent photoactivation of the photosensitizer. Due to wavelength-dependent penetration depth of the photostimulating light, photodynamic therapy in tissues is usually carried out with red light to maximize the effective treatment volume. The main obstacles in using green or blue/violet radiation for photoactivation of most (tetrapyrolic) photosensitizers result from the absorption of light by hemoglobin, melanin, and other tissue constituents. However, this is not a problem for a monolayer of cells in cell cultures. The Soret absorption band located around 400 nm is far more intense than green/red Q absorption bands allowing for reduced exposure to violet/UV light. It was demonstrated for human skin fibroblasts that while 50% lethal light dose (LLD_{50}) is equal to 13.5 and 4.5 J/cm^2 for red (610 nm) and green (500 nm) light, respectively, for violet (410 nm), this drops to 0.35 J/cm^2 (Ref. 22). The cells illuminated with light but not exposed to the photosensitizer exhibited an LLD_{50} equal to >45, >25, and approximately 35 J/cm^2 for red, green, and violet light, respectively.

The selectivity of the PDT cancer treatment comes first of all from selective accumulation of the photosensitizer in abnormal cells and tumor volume,[16,17,20] typically followed by targeted light exposure. There are a few reasons for the selective accumulation of PS in cancer cells. First, there is a higher specific chemical affinity of the PS to those specific cell components, and then, there is also the higher proliferative activity and higher requirement for nutrients for cancer cells. Last, deficiency in expression or activity of some enzymes (e.g., ferrochelatase), observed in abnormal cells, can also play an important role. To enrich the content of hepatocytes in the HepaRG culture, however, selectivity was achieved through spatially controlled UV photoactivation, since having been added to the culture medium, the photosensitizers accumulated in all cells. Targeted light exposure can be achieved *in vitro* by employing laser scanning, but the time required can be considerable due to the sequential cell-by-cell identification and treatment that would be required. However, as described here, significantly higher throughput can be achieved by projecting patterns of UV light to selectively and simultaneously expose unwanted cells once identified automatically. A similar method has been proposed for "directed evolution" and light-mediated selective destruction of cells.[23] Our approach, however, employs a spatial light modulator based on digital light processing (DLP) technology[24] to spatially photoinitiate UV-ALA-PDT mediated destruction of the biliary cells while preserving and effectively enriching the hepatocyte-like cell fraction.

2 Materials and Methods

2.1 *Cell Culture*

2.1.1 *Balb/c 3T3 cells*

Balb/c 3T3 mouse fibroblast cells (American Type Culture Collection; clone A31) were cultured in 75-cm^2 culture flasks (BD-Biosciences 353072) in a humidified incubator (37 °C, 5% CO_2). The culture medium used was composed of Dulbecco's modified Eagle medium (DMEM, Sigma D5796) containing 10% (v/v) newborn calf serum (Gibco 16010-159). After three culture passages, the cells were seeded into 96-well microtiter plates at a density of 3000 cells per well and incubated for 24 h (37 °C, 5% CO_2), after which the culture medium was refreshed before the cells could be used for the experiment.

2.1.2 *HepaRG cells*

HepaRG cells were obtained as preseeded 96-well plates from Biopredic S.A. (Rennes, France). After shipment, the cells were allowed to recover following the supplier instructions using the supplied Low DMSO Containing Medium (After-Shipment Medium; Biopredic, catalogue number MIL475). After 24 h, the cells were further cultured in High DMSO Containing Medium (Biopredic, catalogue number MIL375) until they were used in the experiments.

2.2 *Photosensitizer Substrate*

A solution of 1.19 mM of δ-Aminolevulinic acid (δ-ALA, Sigma-Aldrich) was prepared in, respectively, Balb/c 3T3 cell culture medium and HepaRG cell culture medium.

2.3 *Acquisition of Fluorescence Optical Spectra of Intracellular PpIX*

Spectra of intracellular PpIX, produced by the cells after addition of the photosensitizer substrate, were acquired (1-s acquisition time; dark noise subtracted) using 365-nm excitation (LED model LC-L1 Hammamatsu, Japan; $\lambda_{emi}=365$ nm, PTOT=250 mW) and a back-illuminated, cooled (−15 °C) QE65000 spectrometer (OceanOptics; spectral range 350 to 850 nm, spectral resolution $d\lambda=0.35$ nm) through the optical fiber attached to the output port of the fluorescence microscope.

2.4 *Viability Stainings*

To assess cell viability, cells were stained with propidium iodide (PI) and Hoechst. PI nucleic acid stain (Molecular Probes propidium iodide solid P1304MP, 1 mg/ml) stains only dead cells, since this molecule is excluded from viable cells. Once PI binds to DNA, its fluorescence is enhanced 20- to 30-fold. The PI was observed with an MWG filter cube from Olympus ($\lambda_{exc}=505$ to 560 nm, $\lambda_{emi}>590$ nm).

The blue fluorescence Hoechst Yellow (H) staining (Molecular Probes Hoechst S769121), on the other hand, was used as a marker of viable cells. This dye permeates living cells and binds to all nucleic acids. A DAPI filter (Semrock; $\lambda_{exc}=350$ to 405 nm, $\lambda_{emi}=410$ to 460 nm) was used to image the H staining.

2.5 *Spatial Illuminator*

The heart of the spatial illumination system was a digital micromirror device (DMD). This reflection-type spatial light modulator consisted of a 1024×768 matrix (Discovery 1100 Controller Board and Starter Kit from Texas Instruments) of tiltable micromirrors (13.68 μm square) that were controlled independently by the underlying complementary metal-oxide semiconductor (CMOS) electronics. Binary images, representing the spatial pattern to be projected, were transmitted through a fast USB 2.0 connection from a PC, facilitated by a dedicated software library (Tyrex Services Group Ltd, Austin, Texas).

For the experiments, two instrument configurations were tested. The first, namely, a custom-built parafocal macroscope, was based on a macro zoom lens MS-3 (Meiji Techno, Axbridge, UK). This setup allowed us to perform pilot treatments on the 3T3 cells and let us define critical parameters to further improve the quality and contrast of the projected pattern. To limit the higher diffraction orders observed with the reflective DMD chip, a spatial filtering (iris) had to be introduced in the optical path. With the knowledge obtained from this experiment, we were able to optimize, design, and implement the spatial light projector under an inverted fluorescence microscope (Olympus IX71, Germany). This later microscope setup was used for the actual ALA-PDT treatment on the HepaRG cells. A schematic illustration is presented on Fig. 1.

The light from an ultraviolet photoactivation light source (LED model LC-L1; Hammamatsu, Japan; $\lambda_{emi}=365\pm5$ nm, $P_{TOT}=250$ mW) was expanded to illuminate homogenously the DMD surface. Even though the 365 ± 5-nm radiation does not perfectly fit the absorption band of PpIX, we have decided to use this incoherent light source due to high total irradiance (up to 4600 mW/cm^2 on

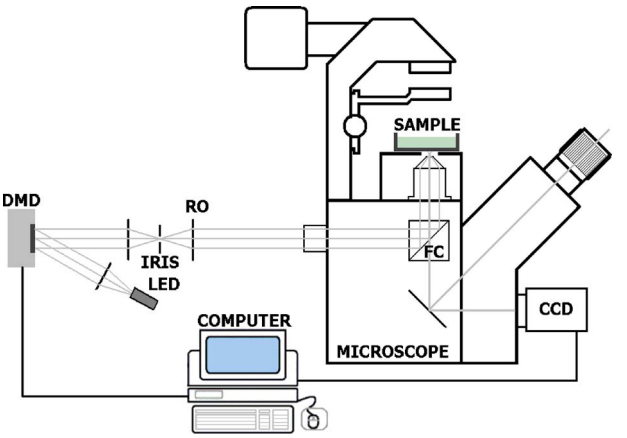

Fig. 1 Schematic of the spatial-projector setup. The light from an ultraviolet photoactivation light source (LED) was expanded to homogenously illuminate the DMD surface. The UV light pattern was projected through relay optics (RO), the spatial filter (iris), and a DAPI filter cube (FC) onto the flat bottom of a plastic well plate.

exit aperture) and the absence of side effects typical for laser sources (laser speckles). The UV light pattern created by reflection from the "on" micromirrors was projected through relay optics (RO), the spatial filter (iris), and through a DAPI filter cube (FC, SemRock Ltd.) onto the flat bottom of a plastic well plate. During the projection, the well plate's cover lid was removed to avoid double reflections that could accidentally photoactivate PpIX-sensitized hepatocyte cells.

For the macroscope setup, the spatial resolution was equal to 3.24 μm/mirror and covered 1024×768 mirrors=3.3 ×2.5 mm area on the sample. The irradiance at the sample, measured with a power meter (Coherent FieldMax II with UV-enhanced OP-2 silicon head) was 16.9 mW/cm^2. For the microscope setup, the contrast of the pattern was enhanced by spatial filtering, and the irradiance at the sample was increased to 184 mW/cm^2. The measured resolution was equal to 1.07 μm/mirror at the sample plane, and the size of illumination field was equal to 1.1×0.8 mm. The light source and conditioning optics used in this study could be optimized to further improve the quality (e.g., resolution and contrast) of the UV-ALA-PDT system.

2.6 *Treatment and Experimental Protocol*

Balb/c 3T3 mouse fibroblast cells were seeded and incubated in the dark for 24 h in medium containing 1.19 mM δ-ALA. After this treatment, a nonuniform checkerboard pattern was projected onto the cell culture by spatially selective UV illumination (at 365 nm). Subsequently, the cells were incubated for 3 h at 37 °C and 5% CO_2, followed by the addition of 1 μL PI and 1 μL H per 100 μL medium. After a period of 5 to 20 min, fluorescence images of PI and H were acquired with an automatic inverted fluorescence microscope IX81 (Olympus, Hamburg, Germany) and CellP (Olympus) software. The PpIX fluorescence spectra and images of endogenous fluorescence were measured on the inverted fluorescence microscope using a U-MWBV2 (Olympus) filter cube with no PI/H staining

The spatially selective photoactivation step consisted of several preparation actions. First, the spatial calibration of the

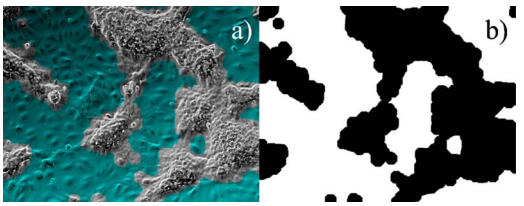

Fig. 2 Automatic analysis of the bright-field image (a) allowed the creation of a mask (b) demarcating the biliary cell ROIs (white) from the hepatocyte regions (black). In image (a), the mask (green) has overlayed the bright-field image. (Color online only.)

illuminator was performed before each experimental session in order to relate the CCD camera image pixel coordinates with the DMD micromirrors coordinates. An automatic detection of regions of interest (ROIs) covered by unwanted biliary cells was performed through computer-based analysis of the bright-field image. This proved effective since the morphology of biliary and hepatocyte cell clusters was quite different, allowing them to be easily distinguished. The automatic ROI identification was achieved by shading correction of the bright-field cell culture image, followed by a series of image processing operations. Briefly, the binary gradient was calculated, and a mask was obtained by dilatation, filling the holes, and segmentation. Further closure of the image was followed by rejecting of small objects and adding a border to the mask. An example is presented in Fig. 2, where a white-light sample image [Fig. 2(a)] overlaps with the mask [Fig. 2(b)] derived from the image. Next, spatially selective illumination was carried to deliver the required light dose to the regions with the unwanted cells.

The image acquisition, system calibration, and DMD projection were controlled by LabView 8.5 (National Instruments) custom-written software, while the automatic image analysis relied on custom-written external MATLAB (2006R, MathWorks, Natick, MA, USA) routines based on standard MATLAB documentation and examples.

3 Results

Initial experiments carried out with Balb/c 3T3 cells showed the effectiveness of the method described here to selectively kill cells in an adherent cell culture. After treatment with the photosensitizer δ-ALA, a nonuniform checkerboard pattern was projected onto the cell monolayer. Only the white squares of the checkerboard pattern were illuminated with UV. As a result, cell death was observed only in those illuminated areas, after viability staining, as shown in Fig. 3. In addition, these initial experiments served to establish and optimize the most effective UV light dose.

The HepaRG cells were more demanding and difficult to handle due to the heterogeneous distribution of the two cell types in the cell culture.

In an initial experiment, the production of PpIX was verified for both hepatocytes and biliary cells after δ-ALA treatment. For this purpose, the (iris) diaphragm of the back UV lamp port of the microscope was closed to form a small UV light spot on the sample [Figs. 4(d) and 4(e)]. Utilizing the dual output port available on the microscope, both fluorescence images and the corresponding fluorescence spectra

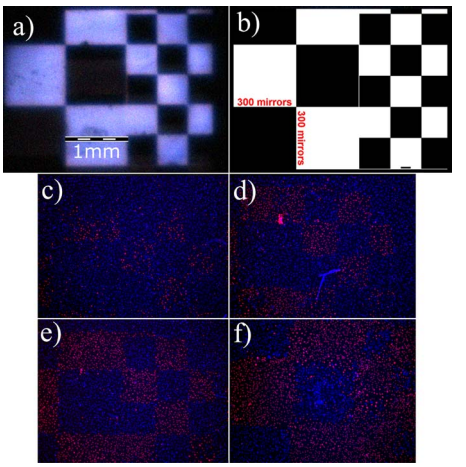

Fig. 3 Checkerboard pattern of UV light projected onto the cell culture (a) and original binary DMD pattern measured on a macroscope (b). Close-ups of microscopic fluorescence images of PI (red fluorescence) and Hoechst (blue fluorescence) stained 3T3 cells incubated with 1.19 mM δ-ALA for 24 h and exposed to patterns with a (c) 2.0, (d) 3.0, (e) 5.1, and (f) 10.2 J/cm^2 UV light dose. The 1-mm scale bar corresponds to the size of the largest rectangle on the pattern and applies to (a) and (c) to (f). (Color online only.)

could be acquired with a CCD camera and a miniature spectrophotometer, respectively. The background signal of the fluorescence images, which most probably came from the autofluorescence of the medium and the optical components, was corrected for by subtracting a broad fluorescence spectrum of a well of the multiwell plate filled with medium alone.

It was observed that the hepatocyte fraction of the cell culture had a much higher production of PpIX when compared to biliary-like epithelial cells. The images presented in Fig. 4 are roughly representative for the HepaRG cell cultures, since the hepatic cell exhibited well-to-well and plate-to-plate variability both in volume and morphology. There are no means to split the cells for independent spectral measurements of biliary and hepatic cells susceptibility to the ALA-PDT treatment. Otherwise, a wide range of studies should be performed, such as PpIX content per cell volume, impact of local chemical environment on this organic fluorophore, which may potentially explain spectral shift on Fig. 4(c) and the kinetics of PpIX production (which we had considered to be a possible way to improve selectivity of ALA-PDT spatially selective killing of biliary cells only). The microscope spectrofluorimetry could be further engaged for spectral characterization of both cell types.

To evaluate the susceptibility of the two cell types to UV-ALA-PDT illumination, a checkerboard pattern was projected onto the δ-ALA–treated HepaRG culture for four different exposure intervals (i.e. 30 s, 60 s, 120 s, 180 s). Figure 5 shows the cell viability for the illuminated and nonilluminated (negative control) areas and provides a qualitative analysis of the light dose dependence of the two cell types.

Due to higher PpIX content, hepatocyte cell clusters showed much higher susceptibility to UV-ALA-PDT treatment, i.e., required lesser light dose to photoinitiate the PDT (Fig. 5). Therefore, illumination of the biliary cell regions had to be precise to avoid any undesirable light leakage. For that purpose, selective killing of biliary cells was following the

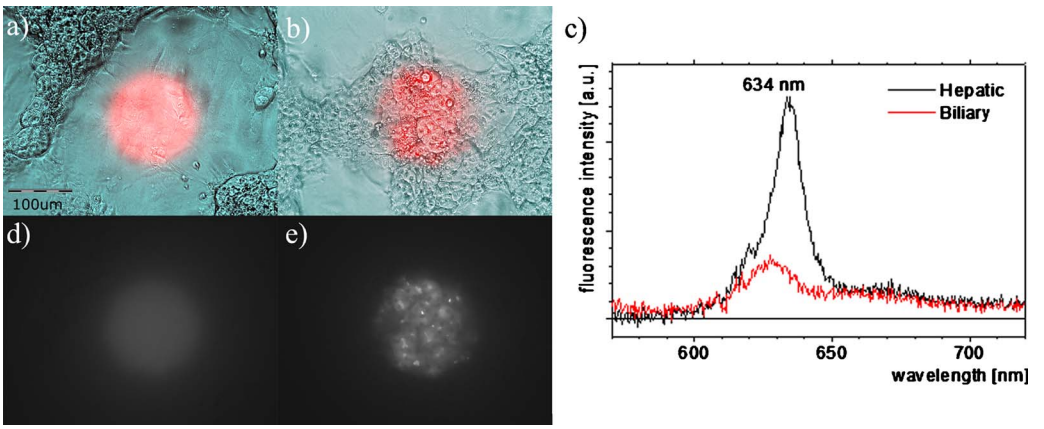

Fig. 4 A quantitative comparison of the fluorescence spectra (c) of PpIX synthesized by biliary cells [(a) and (d)] and hepatocytes [(b) and (e)] cells. The spectra were collected from small spots [(d) and (e)] indicated on bright-field images [(a) and (b)].

algorithm described in Sec. 2.5 and briefly presented in Fig. 2. White-light images of the HepaRG culture [Fig. 2(a)] were acquired after δ-ALA treatment and were then automatically processed to select the ROIs containing only biliary cells, visible as the "flat" regions in Fig. 2(a) and white regions in the binary mask [Fig 2(b)]. The binary mask was scaled and converted to the DLP coordinates. Consequently, at the time of illumination, only these regions were exposed to UV, with the hepatocyte regions being kept effectively in the dark.

The proper experiment was performed on HepaRG cells with four different UV exposure times (60 s, 120 s, 180 s, 240 s) and the same 1.19-mM dose of δ-ALA. The viability of the treated cell culture was again assessed with PI/H staining (Fig. 6). These images demonstrate that through spatially selective photodynamic treatment, one can selectively kill the biliary epithelial cells, preserving the integrity of the hepatocyte population of the HepaRG culture.

4 Discussion

The clear differences in morphology between the clusters of biliary cells and hepatocytes resulted in respective smooth and rough textures in the bright-field image. Thus, the algorithm for automatic generation of a mask comprising biliary ROIs performed very satisfactorily. However, small groups of hepatocytes that did not exhibit the typically rough morphology of larger clusters were wrongly identified at times. Although the fraction of hepatocytes affected was very small, the algorithm could be fine-tuned to achieve a better performance.

In preliminary work, it was quite straightforward to show that at the doses used in this study for UV-ALA-PDT, the UV light itself did not cause any harmful effect to the HepaRG cells. Also, to get some insight into any inherent cytotoxicity of δ-ALA (without UV illumination), a neutral red uptake (NRU) assay was carried out with the 3T3 cell model (data not shown). The IC_{50} value obtained (i.e., the concentration at which cell viability equals 50% of the viability of a control sample) was 5.12 mM, which is 4.3 times higher than the 1.19-mM concentration used in the study presented here. Based on the observation of PI/H stained fluorescence images, the δ-ALA at the concentration of 1.19 mM did not show any cytotoxicity effect in the HepaRG cells.

We have verified that δ-ALA given in excess to the HepaRG cell culture leads to increased PpIX production. The fluorescence intensity observed for the hepatocytes was around 4 to 5 times stronger than that of the biliary cells (Fig. 4). Furthermore, bright small structures are noticeable on the HepaRG fluorescence images [Fig. 4(e)]. Those structures correspond most probably to PpIX accumulation in the bile canaliculi, which would confirm the hepatic transport activity of the HepaRG model.

Figure 5 demonstrates the different susceptibilities of hepatocyte and biliary cells to the UV-ALA-PDT treatment. The treatment at high light dose, i.e., 33 J/cm^2 [Fig. 5(d)] or 22 J/cm^2 [Fig. 5(c)], is lethal to both cell types; however, at a low light dose of 11 J/cm^2 [Fig. 5(b)] or 5.5 J/cm^2 [Fig. 5(a)], it does not affect the biliary cells but is lethal for the hepatocytes. The susceptibility of the HepaRG hepatocytes to the UV-ALA-PDT treatment is at least four times higher than that for biliary cells, which is in line with the PpIX spectra intensities ratio, as presented in Fig. 4(c). We suspect that the higher accumulation of the PpIX observed for the hepatocytes results from higher metabolic activity of these cells in comparison to biliary cells, as well as from the smaller size of the

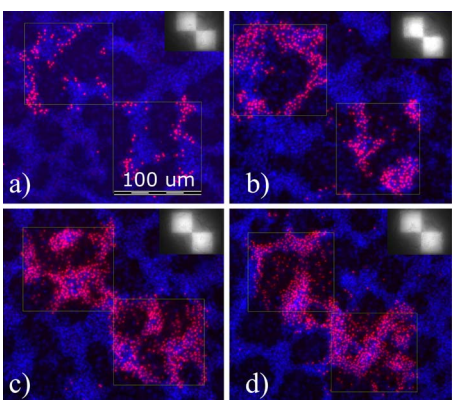

Fig. 5 The response of hepatocytes and biliary cells to the UV-ALA-PDT carried out for (a) 30 s (5.5 J/cm^2); (b) 60 s (11 J/cm^2); (c) 120 s (22 J/cm^2); and (d) 180 s (33 J/cm^2) of UV illumination (184 mW/cm^2). The upper-right insets contain respective UV patterns projected onto the cells.

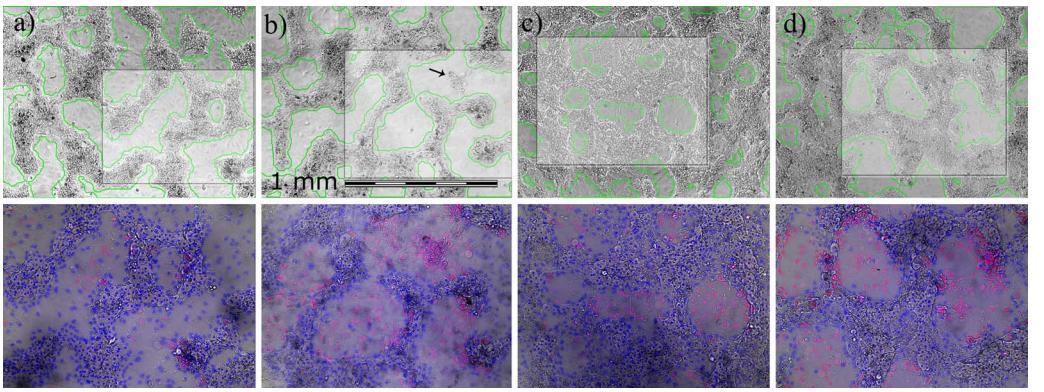

Fig. 6 In the top row, the outlines of the biliary cell ROIs (solid green contours) are overlaid on the associated bright-field images. The spatial extent of the projection is indicated as a partially transparent gray rectangle. In the bottom row are the close-ups of bright-field images overlaid with fluorescence images (red PI and blue Hoechst) of cultures exposed to UV radiation (184 mW/cm^2) for (a) 60, (b) 120, (c) 180, and (d) 240 s (11, 22, 33, and 44 J/cm^2, correspondingly). (Color online only.)

cells leading to a higher concentration of mitochondria per cell volume.

The observed difference in susceptibility should be handled with care while designing and projecting the UV pattern. The areas of biliary cells on the binary mask were reduced by introducing an additional border into the binary mask (Fig. 1). The quality and contrast of the UV light pattern that was projected on the sample was significantly improved in comparison to the initial experiments carried out on Balb/c 3T3 cells. A field stop iris installed in the optical path diminished higher diffractive orders from the DMD chip. Additionally, the well-plate lid was removed during the time of illumination to prevent specular light reflections that can decrease the contrast of the pattern. We have also noticed that polystyrene multiwell plates are not ideal for the UV-ALA-PDT experiments due to the significant light absorption and scattering on the plastic. The use of glassbottomed cell culture plates may improve the quality of this method considerably.

Microscopic observations of the cells for up to two days after the selective killing of the biliary epithelial-like fraction (Fig. 6) did not show any morphological changes of the hepatic colonies. The dead biliary cells did not detach from the surface, and thus no free surface space became available that could induce dedifferentiation of the hepatic-like cells. However, we are aware that biochemical intercell signaling may potentially trigger apoptosis in adjacent cells or influence their behavior. It is known that singlet oxygen generated under UV-ALA-PDT treatment can lead to the activation of stress kinases, such as c-Jun-N-terminal kinase and p38 (Ref. 25). For these reasons, the treated cell culture needs careful examination and further enzymatic and genetic characterization.

While 11 J/cm^2 irradiance [Fig. 6(a)] is not effective, 44 J/cm^2 [Fig. 6(d)] seems to initiate the ALA-PDT for hepatic cells on the borders between the two cells clusters, where the edge of illumination pattern was located. The optimal irradiance 22 to 33 J/cm^2 was found to exclusively kill biliary cells with no injury to hepatic cells, unless these were mistakenly classified by the automatic recognition algorithm to belong to biliary cells cluster [e.g., an island on Fig. 6(b) marked by an arrow].

5 Conclusions

The human hepatoma HepaRG cell line is an *in vitro* cell model used for drug metabolism, hepatotoxicity, genotoxicity, and enzyme induction studies. These cells differentiate into two morphologically different cell types: hepatocyte-like cells and biliary epithelial-like cells. However, variable content and presence of the "contaminating" biliary cells can be regarded as a drawback of the HepaRG culture for some applications. Unfortunately, due to the bipotent properties of the HepaRG cells, there are no known selective culturing conditions or cell sorting methods available that would allow extracting exclusively hepatocyte-like cells. One possible way to selectively purify the hepatocyte-like cell fraction is to eliminate contaminating biliary epithelial-like cells *in situ*.

In this study, we have proposed and implemented a method to enrich the hepatocyte cell fraction in the HepaRG culture. After administration of the heme co-factor precursor δ-ALA in excess (1.19 mM) to the cells, they synthesize high quantities of protoporphyrin IX, which is a naturally occurring photosensitizing agent. Based on automatic bright-field image processing, spatially selective photoactivation ($\lambda_{activation}$ =375 nm, D=22 J/cm^2) of the photosensitizer accumulated in the unwanted cells was performed. A quantitative assay in which the number of dead cells among each cell type is counted could be interesting. However, the H/P images [Fig 6(d)] indicate that the number of dead cells lie almost exclusively within the biliary area of the cell culture. The number of dead hepatocytes is minimal.

Our approach exploited a digital light projector under a fluorescence microscope, which can be further automated toward higher throughput. We believe that this technique can also be successfully employed in specific cell purification of other co-culture models, especially in the area of stem cell culture, where the presence of unwanted phenotypes can be problematic.

References

1. A. Guillouzo, A. Corlu, C. Aninat, D. Glaise, F. Morel, and C. Guguen-Guillouzo, "The human hepatoma HepaRG cells: a highly

differentiated model for studies of liver metabolism and toxicity of xenobiotics," *Chem. Biol. Interact.* **168**, 66–73 (2007).
2. P. Gripon, S. Rumin, S. Urban, J. Le Seyec, D. Glaise, I. Cannie, C. Guyomard, J. Lucas, C. Trepo, and C. Guguen-Guillouzo, "Infection of a human hepatoma cell line by hepatitis B virus," *Proc. Natl. Acad. Sci. U.S.A.* **99**, 15655–15660 (2002).
3. C. Aninat, A. Piton, D. Glaise, T. Le Charpentier, S. Langouët, F. Morel, C. Guguen-Guillouzo, and A. Guillouzo, "Expression of cytochromes P450, conjugating enzymes and nuclear receptors in human hepatoma HepaRG cells," *Drug Metab. Dispos.* **34**, 75–83 (2006).
4. M. Le Vee, E. Jigorel, D. Glaise, P. Gripon, C. Guguen-Guillouzo, and O. Fardel, "Functional expression of sinusoidal and canalicular hepatic drug transporters in the differentiated human hepatoma HepaRG cell line," *Eur. J. Pharm. Sci.* **28**, 109–117 (2006).
5. V. Cerec, D. Glaise, D. Garnier, S. Morosan, B. Turlin, B. Drenou, D. Kremsdorf, C. Guguen-Guillouzo, and A. Corlu, "Transdifferentiation of hepatocyte-like cells from the human hepatoma HepaRG cell line through bipotent progenitor," *Hepatology (Philadelphia, PA, U. S.)* **45**, 957–967 (2007).
6. R. I. Freshney, *Culture of Animal Cells—A Manual of Basic Techniques*, 5th ed., Wiley-Liss Publication, Hoboken, NJ (2005).
7. T. J. Dougherty, C. J. Gomer, B. W. Henderson, G. Jori, D. Kessel, M. Korbelik, J. Moan, and Q. Peng, "Photodynamic therapy," *J. Natl. Cancer Inst.* **90**(12), 889–905 (1998).
8. J. T. H. M. van der Akker and S. B. Brown, "Photodynamic therapy based on 5-aminolevulinic acid: applications in dermatology," in *Photobiology for the 21st Century*, T. P. Coohill and D. P. Valenzeno, Eds., pp. 165–181, Valdenmar Publishing Company, Kansas, USA (2001).
9. T. Hasan, A. C. E. Moor, B. Ortel, and B. W. Pogue, "Photodynamic therapy of cancer," in *Holland Frei Cancer Medicine*, D. Kute, R. Pollock, R. weichselbaum, R. Bast, Jr., T. Granster, J. Holland, and E. Frei, Eds., Chapter 40, pp. 605–6522, Dekker, Inc., Hamilton, Canada (2003).
10. C. Fritsch, K. Lang, W. Neuse, T. Ruzicka, and P. Lehmann, "Photodynamic diagnosis and therapy in dermatology," *Skin Pharmacol. Physiol.* **11**, 358–373 (1998).
11. C. Fritsch and T. Ruzicka, *Fluorescence Diagnosis and Photodynamic Therapy of Skin Diseases*, Springer, Vienna, New York (2003).
12. S. H. Ibbotson, "Topical 5-aminolaevulinic acid photodynamic therapy for the treatment of skin conditions other than non-melanoma skin cancer," *Br. J. Dermatol.* **146**, 178–188 (2002).
13. C. A. Morton, S. B. Brown, S. Collins, S. Ibbotson, H. Jenkinson, H. Kurwa, K. Langmack, K. Mckenna, H. Moseley, A. D. Pearse, M. Stringer, D. K. Taylor, G. Wong, and L. E. Rhodes, "Guidelines for topical photodynamic therapy: report of a workshop of the British Photodermatology Group," *Br. J. Dermatol.* **146**, 552–567 (2002).
14. R. R. Allison, G. H. Downie, R. Cuenca, X. H. Hu, and C. J. H. Childs, "Photosensitizers in clinical PDT," *Photodiagn. Photodyn. Ther.* **1**, 27–42 (2004).
15. E. S. Nyman and P. H. Hynninen, "Research advances in the use of tetrapyrrolic photosensitizers for photodynamic therapy," *J. Photochem. Photobiol., B* **73**, 1–28 (2004).
16. J. C. Kennedy, R. H. Pottier, and D. C. Pross, "Photodynamic therapy with endogenous protoporphyrin IX: basic principle and present clinical experience," *J. Photochem. Photobiol., B* **6**, 143–148 (1990).
17. T. J. Dougherty, "Photosensitizers: therapy and detection of malignant tumors," *Photochem. Photobiol.* **45**, 879–889 (1987).
18. C. J. Gomer, "Preclinical examination of first and second generation photosensitizers used in photodynamic therapy [review]," *Photochem. Photobiol.* **54**, 1093–1107 (1991).
19. R. Bonnett, "Photosensitizers of the porphyrin and phthalocyanine series for photodynamic therapy," *Chem. Soc. Rev.* **24**, 19–33 (1995).
20. B. C. Wilson and M. S. Patterson, "The physics, biophysics, and technology of photodynamic therapy," *Phys. Med. Biol.* **53**, R61–R109 (2008).
21. R. M. Szeimies and M. Landthaler, "Photodynamic therapy and fluorescence diagnosis of skin cancers," *Recent Results Cancer Res.* **160**, 240–245 (2002).
22. D. P. Buchczyk, L.-O. Klotz, K. Lang, C. Fritsch, and H. Sies, "High efficiency of 5-aminolevulinicate-photodynamic tretment using UVA irradiation," *Carcinogenesis* **22**(6), 879–883 (2001).
23. N. W. T. Woodbury, B. P. Bowen, and A. Scruggs, "Computer interfaced scanning fluorescence lifetime microscope applied to directed evolution," U.S. Patent No. 7193706 (2007).
24. L. J. Hornbeck, "Digital light processing™: a new MEMS-based display technology," http://focus.ti.com/pdfs/dlpdmd/117_Digital_Light_Processing_MEMS_display_technology.pdf.
25. L. Xue, J. He, and N. L. Oleinick, "Promotion of photodynamic therapy-induced apoptosis by stress kinases," *Cell Death Differ* **6**, 855–864 (1999).